Journal of Electroanalytical Chemistry 1010 (2026) 120058

Contents lists available at ScienceDirect

Journal of Electroanalytical Chemistry

journal homepage: www.elsevier.com/locate/jelechem

Partial least squares calibration as a tool to overcome intermetallic interactions in the stripping analysis of metal ions: Application to the simultaneous determination of Pb(II), As(III), Cu(II), and Hg(II) using gold screen-printed electrodes

Juan J. Triviño [a,*], Clara Pérez-Ràfols [b,c,**], Núria Serrano [b,c], Verónica Arancibia [a], José Manuel Díaz-Cruz [b,c]

[a] Universidad de Chile, Facultad de Ciencias Químicas y Farmacéuticas, Departamento de Química Farmacológica y Toxicológica, Santiago, Chile
[b] Department of Chemical Engineering and Analytical Chemistry, Universitat de Barcelona (UB), Martí i Franquès 1-11, 08028 Barcelona, Spain
[c] Water Research Institute (IdRA), University of Barcelona (UB), Martí i Franquès 1-11, 08028 Barcelona, Spain

ARTICLE INFO

Keywords:
Stripping voltammetry
Multimetal determination
PLS
Screen-printed gold electrodes

ABSTRACT

This work explores the use of partial least squares (PLS) multivariate calibration to address the issues encountered in multianalyte differential pulse anodic stripping voltammetry (DPASV), particularly those arising from competition among metals for active sites on the working electrode and from the formation of intermetallic compounds. A simple and cost-effective method has been developed for the simultaneous determination of Pb(II), As(III), Cu(II), and Hg(II) ions in aqueous matrices by combining DPASV measurements using a commercial low-temperature gold screen-printed electrode (SPAuE) with a PLS-2 calibration model. The latter employs a central composite design (CCD) together with a new 4D-rotation strategy to ensure homogeneous distribution of concentrations for all four analytes. The methodology exhibits good analytical performance, with linear ranges up to 69 μg/L, R^2 values above 0.99, and repeatability and reproducibility below 8.9% and 11.9%, respectively. Additionally, it significantly improves accuracy compared to univariate calibration, achieving recoveries between 88.8% and 121.7%.

1. Introduction

Many heavy metals are classified as a priority because of their potential health risk. Among them, Pb(II), As(III), Cu(II), and Hg(II) ions have attracted a great deal of attention due to their high toxicity, easy accumulation, and lack of degradability. Although arsenic is not a metal element, its toxicity is similar to that of heavy metals, and the relative density meets the definition of heavy metals [1]. The presence of these metals in many water bodies has caused an alert because it produces severe health problems, such as pulmonary, intestinal, and kidney complications, as well as blindness, cancer, and other complications that may lead to death [2]. The World Health Organization (WHO) established the maximum mass limit of Pb, As, Cu, and Hg in drinking water at 10, 10, 2000, and 6 μg/L, respectively.

Thus, it is important to develop sensitive, rapid, and facile methods for the analysis of these trace ions, taking into particular consideration the simultaneous determination of two or more ions [3]. Anodic stripping voltammetry (ASV) is a powerful electroanalytical technique for the simultaneous determination of metal ions in many different substrate materials at very low concentration levels [3,4]. In addition, ASV can provide useful information on the total metal content, as well as characterization of its chemical forms (e.g., labile fraction). In these measurements, the electrode usually works as a single-electrode sensor, which allows the simultaneous determination of several metal ions when non-overlapped peaks are obtained.

A major drawback in the simultaneous analysis of several metal ions using ASV is the generation of intermetallic compounds or alloys on the working electrode. This happens during the deposition stage, when the different metal ions are reduced to their elemental form and the resulting neutral atoms coexist on the electrode surface (or in the

* Correspondence author.
** Correspondence author at: Department of Chemical Engineering and Analytical Chemistry, Universitat de Barcelona (UB), Martí i Franquès 1-11, 08028 Barcelona, Spain.
E-mail addresses: juantrivino@ug.uchile.cl (J.J. Triviño), claraperezrafols@ub.edu (C. Pérez-Ràfols).

https://doi.org/10.1016/j.jelechem.2026.120058
Received 4 February 2026; Received in revised form 2 March 2026; Accepted 18 March 2026
Available online 19 March 2026
1572-6657/© 2026 The Authors. Published by Elsevier B.V. This is an open access article under the CC BY license (http://creativecommons.org/licenses/by/4.0/).

amalgam, if mercury electrodes are used). Then, certain combinations of different atoms (e.g., Cu + Hg or Cu + Zn + Hg) can strongly interact with each other and get stabilized in the electrode, thus seriously affecting the stripping of these metals to the solution when the anodic potential sweep is applied. This behavior, extensively studied in measurements with mercury electrodes [5,6], can also be observed with carbon-based or metallic working electrodes. As a result, different distortions of the ASV peaks may arise, which can negatively affect the sensitivity and resolution of the method for one or more metals analyzed. Moreover, the effect of mutual competition of metals for active sites on the working electrode surface can promote additional complications in stripping measurements [7].

The minimization of the interferences caused by intermetallic compounds can be achieved in the following ways: adding masking agents that allow the precipitation of interfering ions; adjusting the electrolyte composition to separate those substances with similar potential; changing the deposition potential to distinguish target ions from interfering ones; and adding a modifier to the electrode surface to repel interfering anions [8].

An alternative strategy is the use of chemometric methods for the multivariate calibration in the presence of such interferences [9–13]. These methods can be linear, such as partial least squares (PLS), or non-linear, such as support vector machine (SVM) and artificial neural networks (ANN). Although non-linear methods are more powerful than linear ones, in the analysis of intricate data sets, linear methods, and especially PLS, are preferred when the behavior of the system is not far from linearity because they are much faster and simpler, do not require a deep expertise in chemometrics to build calibration models, and can be easily reproduced by other researchers using standard software. This is why, in our case, the first choice was PLS, and the validity of such approach has been confirmed by the consistency of the results described below.

In this work, multivariate calibration by PLS has been applied to the simultaneous determination of the four metal ions Pb(II), Cu(II), As(III), and Hg(II) by DPASV in aqueous samples using a commercial screen-printed gold electrode (SPAuE). These analytes have been chosen not only for their high environmental relevance, but also for the problems caused in stripping measurements by the formation of intermetallic compounds and the competition for the active sites on the electrode surface. Taking this system as a model, PLS calibration has been tested as a valuable alternative to the poor analytical performance of the simultaneous determination of analytes by ASV and classical univariate calibration when the interactions between reduced atoms in the electrode play a significant role. Also, a new methodology has been developed for the experimental design, where a central composite design (CCD) of 4 variables (the concentrations of all four metal ions) has been rotated in 4 dimensions to get a more homogeneous distribution of the concentrations of every analyte. Beyond these aspects, the novelty of this work lies primarily in demonstrating that PLS multivariate calibration can successfully overcome the strong intermetallic interactions and competition for electrode active sites that typically limit the simultaneous determination of metal ions by ASV. Unlike previous studies, where these interactions have been reported as a major barrier to achieving reliable multi-analyte quantification, this work shows that PLS can effectively address such limitations, demonstrating that robust multi-analyte determination is achievable under conditions where classical univariate calibration fails. Moreover, the work shows that the possible losses of linearity caused by intermetallic compounds do not hinder the application of a simple and popular linear method such as PLS, instead of a more sophisticated non-linear approach such as artificial neural networks or support vector machine. In addition, the use of a four-variable central composite design rotated in four dimensions provides a more balanced distribution of analyte concentrations, supporting the robustness of the calibration model.

2. Experimental

2.1. Reagents

Standard solutions of Pb(II), Cu(II), As(III), and Hg(II) were prepared by diluting commercial standards containing 1000 mg/L from Merck (Certipur, Darmstadt, Germany). All the other chemicals (nitric acid, hydrochloric acid, phosphoric acid, boric acid, acetic acid, and sodium hydroxide) were of Suprapur grade (analytical reagent grade) and obtained also from Merck. Milli-Q water (reference A+, Millipore, France) was employed for sample preparation, dilution of reagents, and rinsing purposes.

2.2. Instrumentation

Voltammetric measurements were performed using a μAutolab System Type III (EcoChemie, The Netherlands) coupled to a Metrohm 663 VA stand (Metrohm, Switzerland) and controlled by GPES software (version 4.9.007, Ecochemie). The electrochemical cell consisted on a low-temperature SPAuE acquired from Metrohm-Dropsens (Oviedo, Spain, reference DRP-C220BT, batch E0014485), which contains a 4 mm gold working electrode (WE), a silver reference electrode (RE), and a gold auxiliary electrode (AE). Chemometric analysis was performed by Eigenvector's PLS-Toolbox software [14], and further data processing and visualization was carried out using Microsoft Excel, GraphPad Prism, and Matlab [15].

2.3. Voltammetric determination of metal ions

Prior to any voltammetric analysis, SPAuEs were activated by performing 30 cycles by cyclic voltammetry (CV) from −0.1 to +1.1 V at 100 mV/s in 0.5 mol/L H_2SO_4. Unless otherwise stated, differential pulse anodic stripping voltammetric (DPASV) measurements using an activated SPAuE were performed applying an accumulation potential (E_{acc}) of −0.4 V for 30 s under stirring and scanning the potential from −0.5 to +0.6 V using 100 mV as pulse amplitude, 10 ms as pulse time, 8 mV as voltage step and 100 ms as voltage step time. All voltammetric measurements were carried out without deaeration and a preconditioning step of 30 s at +0.6 V was applied prior to the DPASV measurement to remove any metals adsorbed onto the electrode surface.

Individual and simultaneous univariate calibrations were performed increasing the concentrations of Pb(II), As(III), Cu(II) and Hg(II) in 0.1 mol/L of HCl as supporting electrolyte. Analytical parameters were calculated from three independent calibration curves.

The accuracy of the method was assessed through the voltammetric analysis of two separate samples prepared in 0.1 mol/L HCl and containing different values and ratios of metal ions. Specifically, sample A contained 11.0 μg/L Pb(II), 21.0 μg/L As(III), 31.0 μg/L Cu(II) and 16.0 μg/L Hg(II); and sample B contained 52.5 μg/L Pb(II), 16.0 μg/L As(III), 36.0 μg/L Cu(II) and 23.5 μg/L Hg(II). Samples A and B were analyzed in triplicate by means of the standard addition method. For this purpose, 10 mL of sample were placed into the voltammetric cell and the DPASV signal was recorded. Subsequently, four aliquots of metal ions standard solutions (14 μL of 5.0 mg/L) were further added into the cell and the respective voltammetric curves were recorded.

For multivariate calibration, a PLS-2 model was built using the entire voltammogram as X block and the concentration values of the four metal ions as Y block. For this purpose, a total of 39 samples containing different values and ratios of metal ions were prepared in 0.1 mol/L HCl and distributed among the calibration (25 samples, 64%) and validation (14 samples, 36%) sets. The concentration values employed for each sample are reported in Table S1.

In order to build the PLS-2 model, voltammetric signals were first pretreated by means of variance (std) scaling to account for different noise magnitudes between samples. A total of 7 LVs were selected for the model according to a compromise in the first minimum of root mean

square error provided by cross validations based on 'leave one out' strategy.

The accuracy of the method was then evaluated towards samples A and B by employing the developed model to predict the concentrations of metal ions in those samples (external validation).

3. Results and discussion

3.1. Optimization of the voltammetric method

DPASV measurements were first optimized looking for a good resolution of the four considered metal ions as well as clearly defined voltammetric peaks. In this context, pH and supporting electrolytes are two parameters with a significant effect onto the shape and size of ASV peaks. Fig. 1A shows, for a solution containing 48.1 μg/L of each metal ion, the effect of pH variation using Britton-Robinson buffer from pH 1.71 to 4.91. In general, metal peaks increase as the pH of the solution becomes more acidic. In fact, three well-defined anodic peaks for Pb(II), Hg(II) and As(III), as well as a small peak associated to Cu(II), can be observed under the most acidic initial conditions. Nevertheless, the four voltammetric signals were not completely separated and thus, the effect of the supporting electrolyte was investigated. Several mineral acids (H_2SO_4, H_3PO_4, HCl, $HClO_4$, and HNO_3) were studied as supporting electrolytes, always considering an acid concentration of 0.1 mol/L and 48.1 μg/L of each metal ion (Fig. 1B). HCl was selected as the optimal supporting electrolyte because it was the only acid that provided a significant signal for Cu(II) and still maintained reasonably well-resolved voltammetric peaks for the remaining metal ions.

Next, the influence of the E_{acc} was examined for a solution containing 48.1 μg/L of each metal ion over the E_{acc} range from 0 to −1 V, considering an accumulation time (t_{acc}) of 30 s (Fig. 1C). As expected, metal signal initially increased as E_{acc} became more negative. Nevertheless, E_{acc} more negative than −0.4 V resulted in greater background currents, the generation of nonspecific peaks, and even interferences due to the formation of bubbles on the electrode surface, which are attributable to the reduction of protons to molecular hydrogen, even more so considering the strongly acidic medium. Thus, an E_{acc} of −0.4 V was selected for further experiments. Then, the effect of t_{acc} was also studied considering a t_{acc} up to 300 s. As observed in Fig. 1D, longer t_{acc} favored the competition among metal ions for the active sites on the electrode surface, resulting in an increase of Cu(II) signal in detriment to As(III) peak. Thus, 30 s was selected as a compromise t_{acc} for the simultaneous determination of the four considered metal ions.

3.2. Individual and simultaneous univariate calibrations

The univariate calibration of each metal ion was first evaluated individually in 0.1 mol/L HCl using a SPAuE by the consecutive measurement of increasing concentrations in the range (5.0–454.5 μg/L). The evolution of DPASV signals of each metal ion when the concentration individually increases is displayed in Figs. 2A-D. As it can be seen, well-defined voltammetric peaks were obtained for all analyzed metal

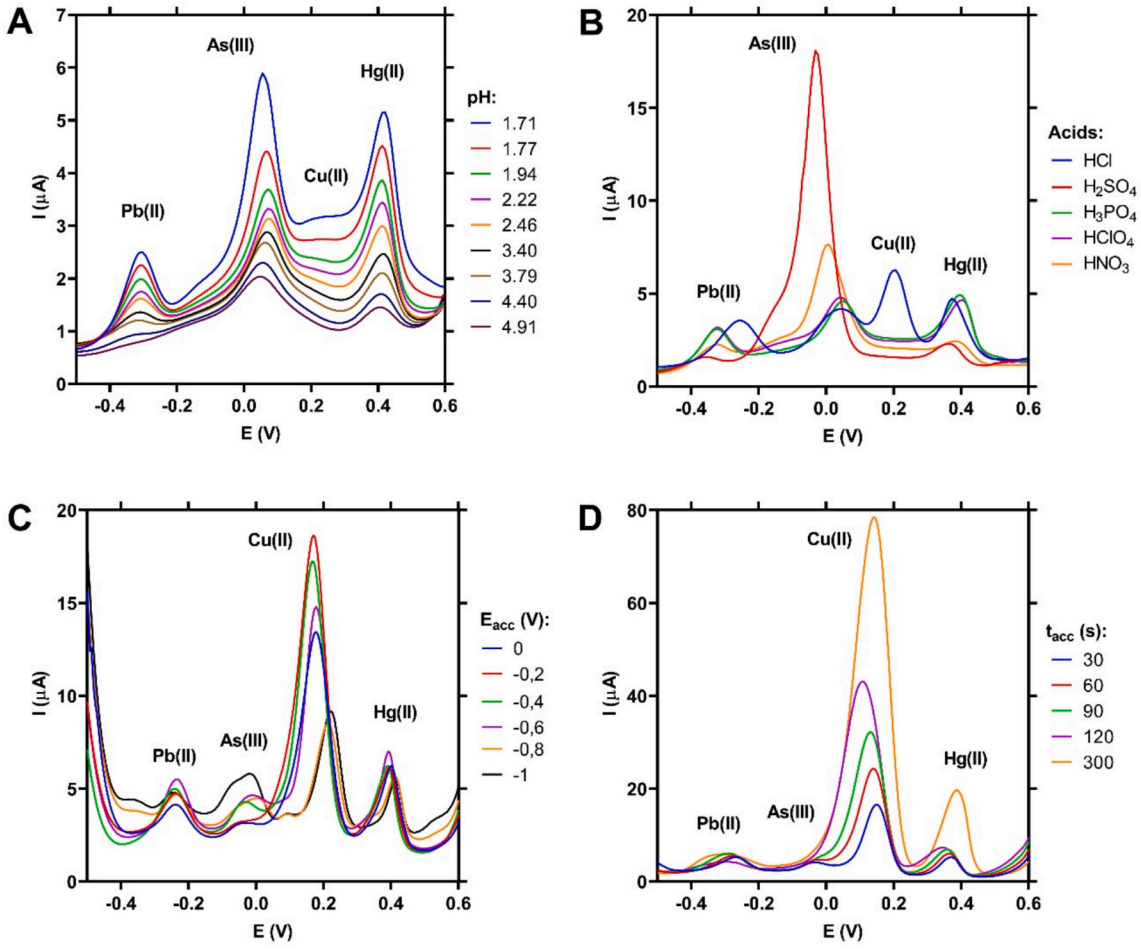


Fig. 1. Optimization of different parameters for the DPVASV determination of 48.1 μg/L of Pb(II), As(III), Cu(II) and Hg(II) using a SPAuE. **(A)** Effect of pH employing a Britton-Robinson buffer with an E_{acc} of −1.0 V and a t_{acc} of 30 s; **(B)** effect of supporting electrolyte considering a 0.1 mol/L acid concentration and with an E_{acc} of −1.0 V and a t_{acc} of 30 s; **(C)** effect of accumulation potential in 0.1 mol/L HCl and with a t_{acc} of 30 s; **(D)** effect of accumulation time in 0.1 mol/L HCl and with a E_{acc} of −0.4 V.

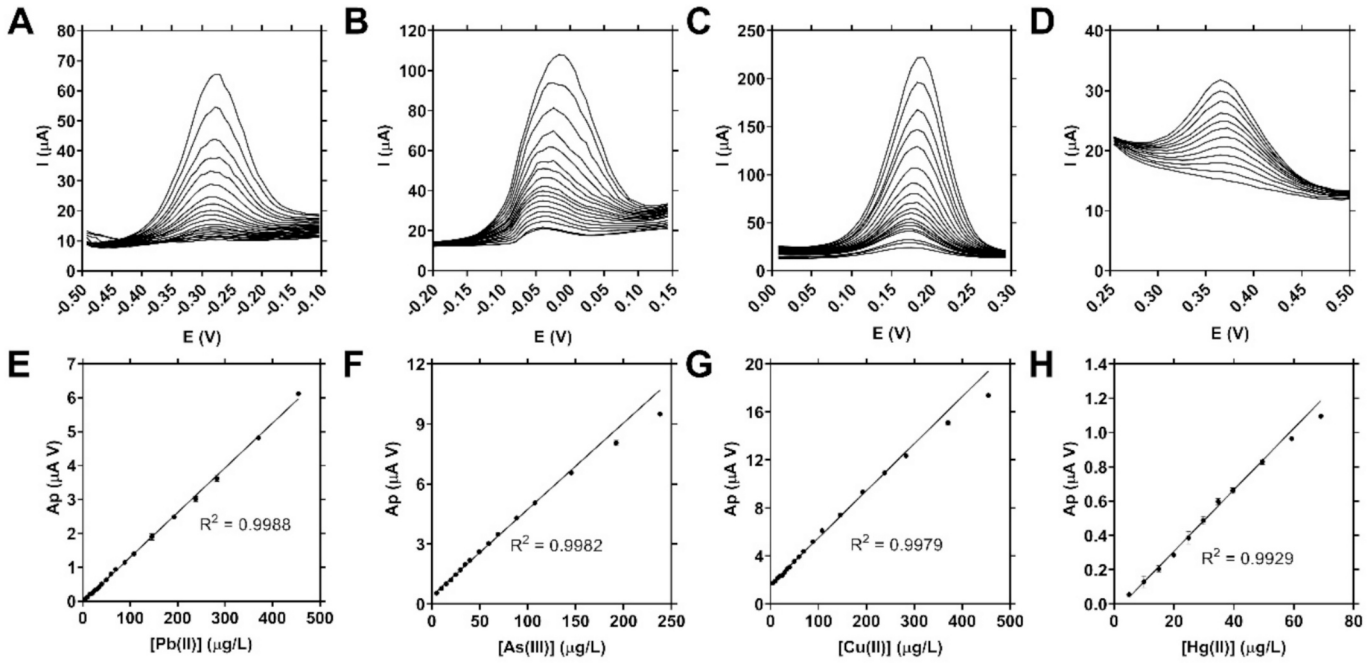


Fig. 2. Individual anodic stripping voltammograms of Pb(II) (A), As(III) (B), Cu(II) (C) and Hg(II) (D); and their respective calibration plots (E), (F), (G) and (H) in 0.1 mol/L HCl using an SPAuE.

ions over the considered concentration range. The obtained calibration curves (Figs. 2E-H) were employed to calculate the main analytical parameters (Table 1): sensitivity, correlation coefficient, limit of detection (LOD), limit of quantification (LOQ) and linear range, for Pb (II), As(III), Cu(II) and Hg(II). Sensitivities were established from the slopes of calibration curves between peak area (μA V) and target metal ion concentration, with As(III) exhibiting the highest sensitivity. For computing LOD and LOQ of target metal ions, the formula considered was three and ten times, respectively, the standard deviation of the intercept divided by the slope of the calibration curve [16]. The obtained LODs ranged from 1.6 to 3.1 μg/L depending on the metal ion considered, with As(III) yielding the lowest LOD. Linear range was stated from the LOQ up to the highest concentration that showed a linear response. Excellent linear correlations between peak area and analyte concentration were obtained for all compounds studied. The calibration ranges extended up to 454.5 μg/L for Pb(II), 145.6 μg/L for As(III), 283.0 μg/L for Cu(II) and 49.5 μg/L for Hg(II). The analytical parameters obtained for the determination of the target ions are comparable to those typically reported in the literature for gold electrodes (Table 4 in ref. 3). This consistency indicates that the developed method performs within the expected range of accuracy and sensitivity, confirming its reliability for individual quantitative analysis.

Additionally, to evaluate whether the simultaneous presence of Pb (II), As(III), Cu(II) and Hg(II) could introduce mutual interferences affecting their individual analytical performance, a simultaneous calibration of the four metal ions was conducted using DPASV with SPAuE. This approach aimed to determine if signal overlap, competitive adsorption, formation of intermetallic compounds or other effects arising from their coexistence might compromise the accuracy or sensitivity of the measurements, which could ultimately limit their applicability for the quantitative analysis of the target compounds (Fig. 3). Well-defined peaks without signal splitting were obtained for Pb (II), As(III), Cu(II) and Hg(II) on SPAuE in the considered concentration range (5.0–454.5 μg/L). Table 1 shows the calibration data for this simultaneous determination. Sensitivities, expressed as the slope of the simultaneous calibration plots for Pb(II), As(III), Cu(II) and Hg(II), exhibit distinct behavior depending on the metal ion under study. The sensitivities obtained from the calibration plots for Pb(II) showed no

Table 1
Analytical figures of merit for the individual and simultaneous determination of Pb(II), As(III), Cu(II) and Hg(II) using a SPAuE in 0.1 M HCl. Standard deviations are denoted by parenthesis.

	Pb(II)	As(III)	Cu(II)	Hg(II)
Individual determination				
Sensitivity (μA V L/μg)	13.16 (0.08)	43.2 (0.4)	39.2 (0.3)	17.9 (0.4)
R^2	0.9988	0.9982	0.9979	0.9929
Linear range (μg/L)[a]	10.2–454.5	5.3–145.6	9.5–283.0	6.1–49.5
LOD (μg/L)	3.1	1.6	2.9	1.8
Simultaneous determination				
Sensitivity (μA V L/μg)	10.1 (0.1)	22.2 (0.4)	28.6 (0.2)	7.89 (0.06)
R^2	0.9962	0.9940	0.9980	0.9977
Linear range (μg/L)[a]	5.8–88.4	6.6–69.0	12.7–454.5	14.0–454.5
LOD (μg/L)	1.7	2.0	3.8	4.2
Repeatability (RSD%; $n = 25$)	7.6	3.3	6.2	8.9
Reproducibility (RSD%; $n = 5$)	11.9	8.1	10.3	10.4

[a] The LOQ is the lowest value of the linear range.

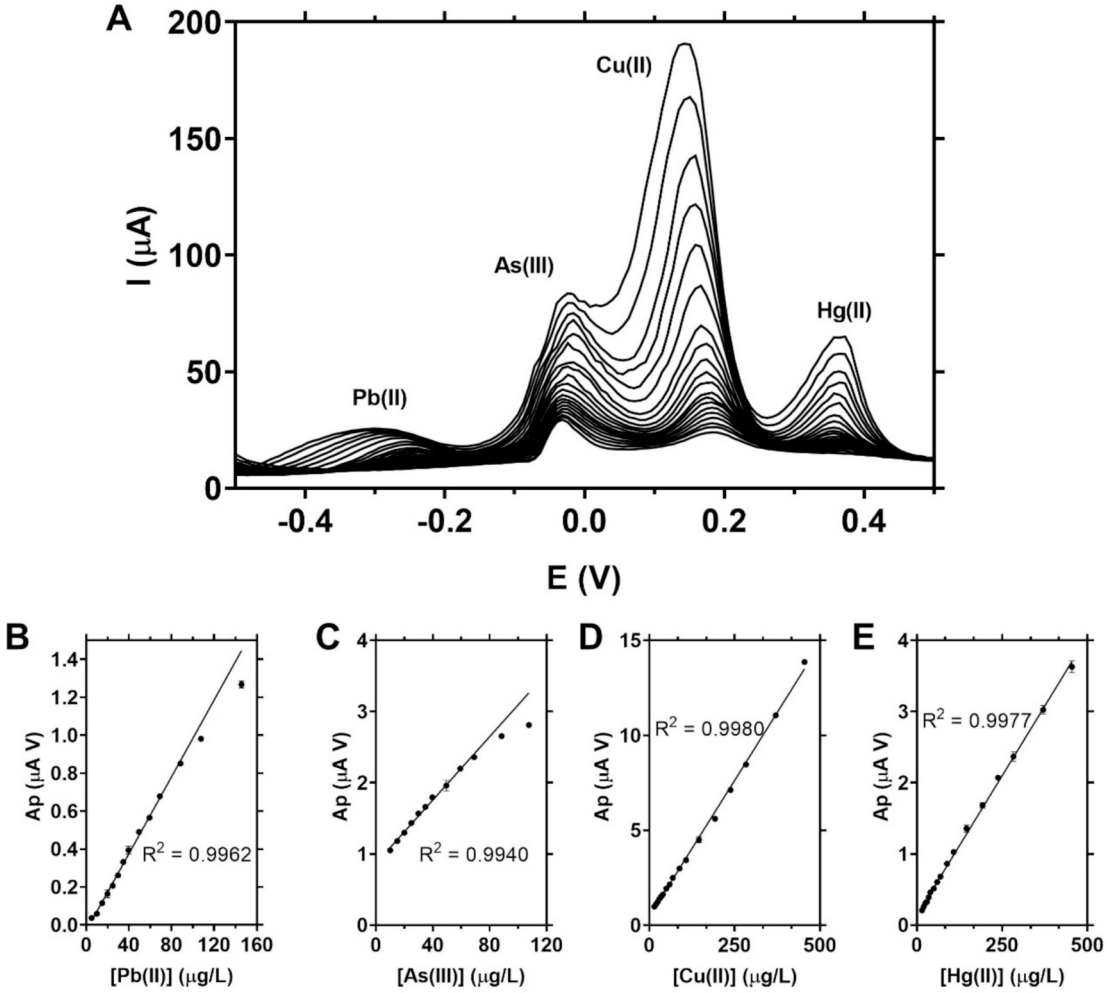


Fig. 3. (A) Anodic stripping voltammograms of a mixture of Pb(II), As(III), Cu(II) and Hg(II); and their respective calibration plots (B), (C), (D) and (E) in 0.1 mol/L HCl using a SPAuE.

substantial variation compared to those achieved in its individual determination. For Cu(II), a slight but not significant decrease in sensitivity was observed. In contrast, for As(III) and Hg(II), the sensitivities were approximately half of those recorded under individual determination conditions, indicating a more pronounced influence of simultaneous analysis on these ions. Regarding the linear ranges, notable differences were observed compared to the individual calibrations. The calibration ranges were significantly shorter for Pb(II) and As (III), whereas, in contrast, the linear ranges for Cu(II) and Hg(II) were considerably broader. The obtained results can be explained, on the one hand, by the fact that during the deposition step a negative potential is applied to the gold electrode, which promotes the reduction of Hg(II) ions in solution and their deposition onto the electrode surface as a gold–mercury amalgam (Au—Hg). Subsequently, As(III) and Cu(II) may also be reduced and co-deposited, reacting with the amalgam to form intermetallic compounds such as Au–Hg–As and Au–Hg–Cu. On the other hand, previous studies have demonstrated that the determination of As(III) by ASV is significantly influenced by interference from several metals. These interferences occur mainly through two mechanisms: (i) the formation of binary intermetallic compounds with arsenic, notably Cu(II) and Se(IV), which produce Cu_3As_2 and As_2Se_3; and (ii) competition for adsorption sites on the gold surface by ions such as Sb(III), Bi(III), Hg (II), Cu(II), and Pb(II), even without forming intermetallic compounds [17]. Among these ions, Cu(II) is regarded as the most critical interferent because it can form Cu_3As_2 during the preconcentration step [18], severely compromising ASV measurements even when Au nanoparticles are used. This issue has been reported for various gold-based electrodes, such as polycrystalline Au electrodes, which promote intermetallic formation and are therefore unsuitable for As(III) detection in the presence of Cu(II), as reported by several authors [19].

The LODs and LOQs obtained from the joint calibrations were of the same order as those provided by the individual calibrations for all studied metal ions, ranging from 1.7 to 4.2 μg/L.

The repeatability and reproducibility of the developed ASV method using an SPAuE were evaluated through joint calibrations (Table 1). ASV measurements were performed for 29.9 μg/L Pb(II), As(III), Cu(II), and Hg(II) in 0.1 mol/L HCl. Repeatability was assessed using the same SPAuE unit over twenty-five consecutive measurements, yielding RSDs between 3.3% and 8.9%, depending on the metal ion. Reproducibility, determined using five different SPAuE units, produced RSDs ranging from 8.1% to 11.9%, again varying with the analyte. These values are consistent with those typically reported for bare commercial SPEs in analytical applications [20–22].

To assess the accuracy of the developed ASV method using an SPAuE, the simultaneous determination of Pb(II), As(III), Cu(II), and Hg(II) was carried out in two synthetic samples (Sample A and B) prepared in 0.1 mol/L HCl and containing different concentrations and ratios of the metal ions (see Section 2.3 for details). Each sample was analyzed in triplicate using the standard addition method. As shown in Fig. 4A for Sample A, the voltammograms displayed well-defined peaks and a performance comparable to that obtained during the simultaneous calibration of the target metal ions. The corresponding calibration

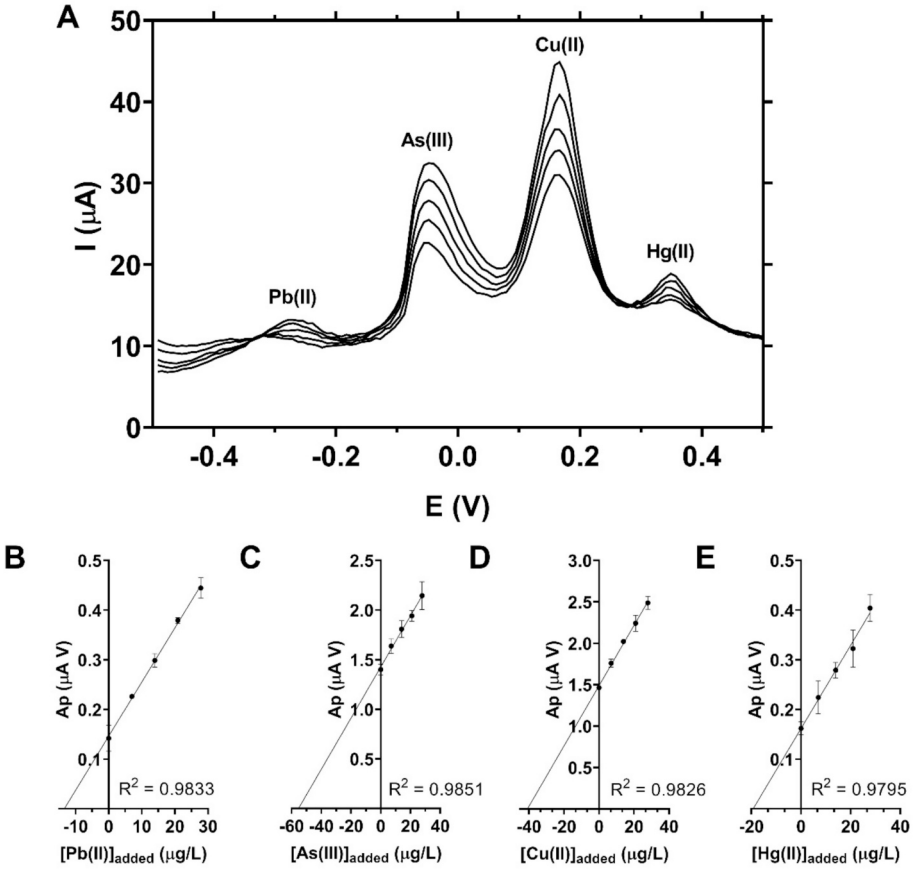


Fig. 4. (A) Anodic stripping voltammograms of Sample A (a mixture of Pb(II), As(III), Cu(II) and Hg(II) in 0.1 mol/L HCl) using a SPAuE; and their respective standard addition plots (B–E).

Table 2
Total concentrations of Pb(II), As(III), Cu(II) and Hg(II) determined in two synthetic samples (Sample A and B) prepared in 0.1 mol/L HCl using a SPAuE. Standard deviations are denoted by parenthesis.

	Pb(II)	As(III)	Cu(II)	Hg(II)
Sample A				
C_{added} (μg/L)	11.0	21.0	31.0	16.0
$C_{determined}$ (μg/L)	13.4 (2.4)	55.3 (10.8)	40.9 (3.1)	21.9 (3.6)
RSD (%)	17.9	19.5	7.6	16.4
Relative error (%)	21.8	163.3	31.9	36.9
Recovery (%)	121.8	263.3	131.9	136.9
Sample B				
C_{added} (μg/L)	52.5	16.0	36.0	23.5
$C_{determined}$ (μg/L)	29.1 (2.0)	36.6 (5.2)	53.1 (14.1)	27.8 (3.9)
RSD (%)	6.9	14.2	26.6	14.0
Relative error (%)	44.6	128.8	47.5	18.3
Recovery (%)	55.4	228.8	147.5	118.3

curves (Fig. 4B-E) demonstrated good linearity in all cases. Similar behavior could be observed for Sample B. However, as observed in Table 2, very large relative error values were obtained, particularly for As(III), reaching 163.3% for sample A and 128.8% for sample B. Regarding the recoveries, all values for sample A exceeded 100%, with an aberrant 263.3% recovery for As(III). In the case of sample B, where the added Pb(II) concentration was much higher than in sample A, the Pb(II) recovery dropped to only 55.4%, while As(III) again showed an anomalously high recovery (228.8%). For the remaining metal ions, recoveries were consistently above 100%.

Based on these results, the use of this method for the simultaneous univariate determination of these metal ions is not advisable, as mutual interferences significantly compromise their quantitative analysis.

3.3. Multivariate calibration

Considering that univariate calibration by means of the standard addition method was not able to successfully quantify the four analytes due to competition between metal ions and the formation of intermetallic compounds, an alternative strategy was considered based on multivariate calibration. In particular, a PLS-2 model was first calibrated and then validated prior to its application to samples A and B.

In order to work with a moderate number of samples that consider different ratios between metal ions, a central composite design (CCD) was chosen for the calibration set and a cubic configuration was used for the validation set, both submitted to an axis rotation to get a higher diversity of concentrations. Fig. S1 illustrates such experimental design. As four dimensions cannot be visualized in conventional graphics, Fig. S1A shows the analogous design with three variables/concentrations: the calibration set (in blue color) is made of 15 samples combining a cube (or a parallelepiped) and a star, and the validation set (in red color) is made of 8 samples contained in a cube (or a parallelepiped). The concentrations of the samples in a CCD design for any number of variables can be easily computed using the function 'ccdesign' by Matlab [15]. However, if these designs are parallel/perpendicular to the coordinate axis, the concentrations employed for every analyte are considerably repeated, i.e., only 5 concentrations for the calibration set and just 2 for the validation set (of course, with different concentrations of the rest of analytes). This is illustrated by Fig. S1B, which shows a 'self-plot' of the concentration of a particular analyte versus this same concentration: only 5 blue points are seen, which accumulate many points which differ in the concentration of the other analytes not depicted. If a

new set of axes is created by rotation of the previous one or if tilted parallelepipeds are built, a greater diversity of concentration is produced. With a proper selection of the rotation or tilt angle it is possible to visualize different concentrations for all calibration and validation samples, i.e., 15 blue points and 8 red points (Fig. S1C). In the case of four analytes, the 4D design implies 25 and 16 samples for the calibration and the validation set, respectively, and again a design parallel/perpendicular to the coordinate axis would produce a high repetition of concentrations, once more 5 blue points and 2 red points (Fig. S1D). Thus, a similar rotate/tilt strategy should produce a more spread set of concentrations. In this work we have used a rotation of the 4 axes in a 4D space, which implies 6 rotations of coordinates (with respect to the planes xy, xz, xt, yz, yt and zt) as described in [23,24]. Rotations were made with a home-made Matlab program and, after trying different angles, a value of 0.35 rad was chosen as optimal to obtain a similar spreading of the values of concentrations for all four analytes. Figs. S1E–H show the results of this strategy, which generates 18 different concentration values for the calibration set among the 25 calibration samples (in blue) and 12 different concentration values for the validation set, out of 16 validation samples (in red). After unifying too close values, the concentrations yielded by this design were adapted to the linear ranges obtained in the individual calibrations of all four analytes, as well as to the characteristics of available solutions and pipettes. As a result, Table S1 shows the concentration that were finally employed to prepare the sets of calibration and validation samples. It should be pointed out samples A and B were removed from the original validation subset to test as external validation, thus resulting in a validation subset with 14 samples.

Under optimal SPAuE electrode conditions, measurements were carried out in random order and produced the calibration and the

Table 3
Main parameters of the regression lines obtained in the comparison between predicted vs. expected values of the training and validation subsets for Pb(II), As (III), Cu(II) and Hg(II) (ranges calculated at the 95% confidence level). The standard deviations are denoted by parenthesis.

	Pb(II)	As(III)	Cu(II)	Hg(II)
Calibration subset				
Slope	0.99 (0.02)	0.99 (0.02)	0.91 (0.06)	0.97 (0.04)
Intercept (μg/L)	0.4 (0.8)	0.3 (0.8)	3 (2)	1 (1)
R^2	0.988	0.986	0.900	0.968
RMSE[a] (μg/L)	1.68	1.82	4.82	2.73
Validation subset				
Slope	1.04 (0.06)	1.02 (0.04)	0.9 (0.1)	0.88 (0.07)
Intercept (μg/L)	-1 (2)	-1 (1)	2 (4)	4 (2)
R^2	0.959	0.985	0.844	0.934
RMSE[a] (μg/L)	2.60	1.74	5.70	3.66

[a] RMSE: Root mean square error.

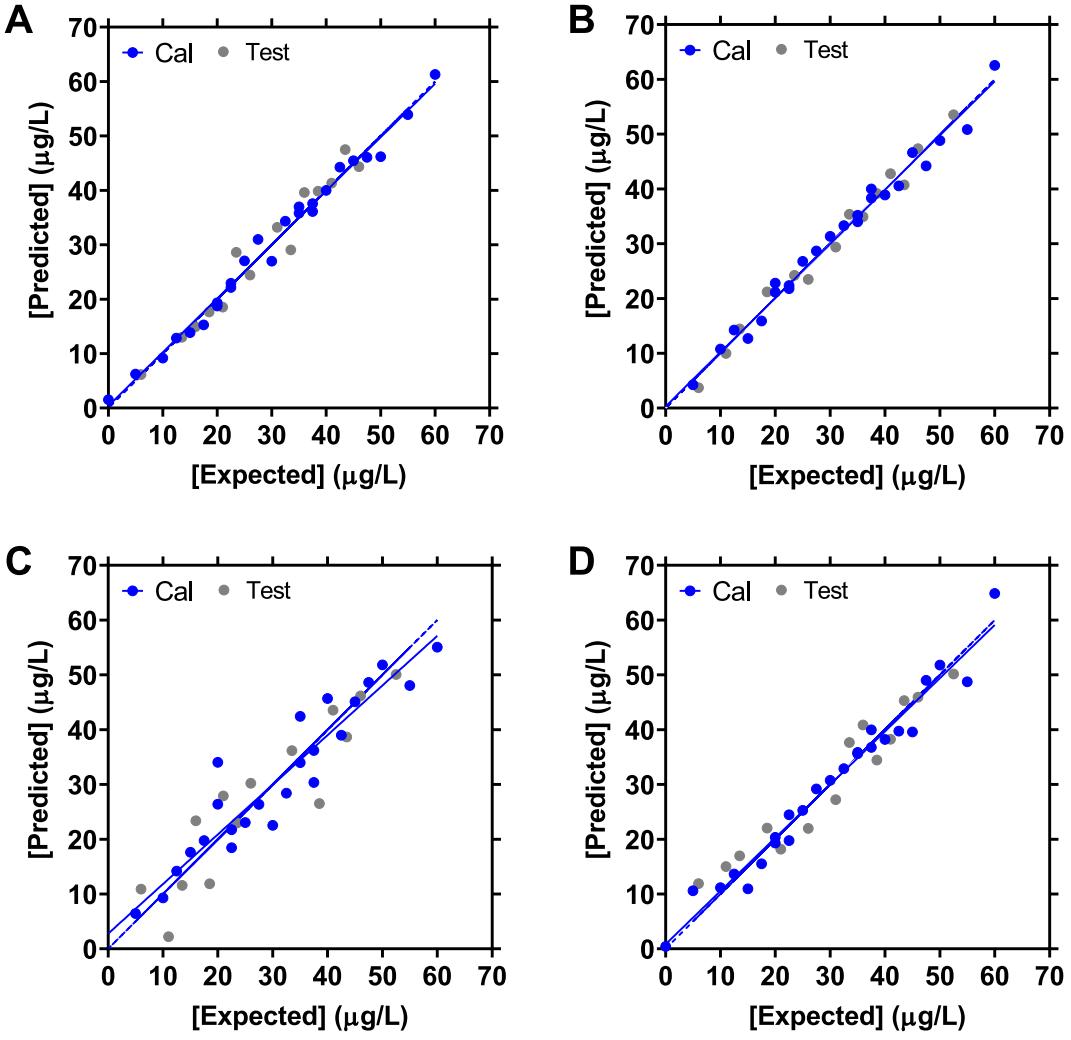


Fig. 5. Comparison graphs of predicted vs. expected concentrations obtained using a SPAuE for Pb(II) (A), As(III) (B), Cu(II) (C) and Hg(II) (D) for training set (blue) and test set (grey). Dashed line represents theoretical diagonal line (y = x). (For interpretation of the references to color in this figure legend, the reader is referred to the web version of this article.)

Table 4
Results for the determination of Pb(II), As(III), Cu(II), and Hg(II) in spiked water samples A and B by means of PLS-2 model.

	Pb(II)	As(III)	Cu(II)	Hg(II)
Sample A				
C_{added} (μg/L)	11.0	21.0	31.0	16.0
$C_{determined}$ (μg/L)	11.2	18.7	37.5	17.6
Relative error (%)	2.2	11.2	20.9	9.8
Recovery (%)	102.2	88.8	120.9	109.8
Sample B				
C_{added} (μg/L)	52.5	16.0	36.0	23.5
$C_{determined}$ (μg/L)	56.6	19.5	33.4	21.7
Relative error (%)	7.7	21.7	7.3	17.7
Recovery (%)	107.7	121.7	92.8	92.3

validation data matrices shown in Fig. S2. Different pretreatments of the raw data (voltammograms) were evaluated and the "Variance (Std) Scaling" pretreatment yielded the best parameters, such as calibration R^2, prediction, and cross-validation. As indicated by the software, this method is almost identical to automatic scaling and is used for the same reason (when noise is expected to be proportional to the standard deviation of the variables); however, this method does not center the data. Another advantage of using this pretreatment is that it does not have adjustable parameters, allowing for a "universal" application to the input data.

Comparison graphs of obtained vs expected concentrations for the four considered metal ions are shown in Fig. 5, and the main regression parameters, as well as the root mean square error (RMSE) are reported in Table 3, both for the calibration and validation subset. As it can be observed, good linearity was obtained in all cases, with slopes and correlation coefficients close to 1, intercepts close to 0 and low RMSE values. Out of all the considered metal ions, the best results were obtained for Pb(II) and As(II). Nevertheless, even in the case of Cu(II) and Hg(II), for which sensitivity and/or linear range significantly varied from individual to simultaneous univariate calibration, PLS-2 was able to procure successful calibration and validation parameters.

After its successful calibration and validation, the developed PLS-2 model was applied to samples A and B in order to compare its prediction ability with that obtained in univariate calibration. As observed in Table 4, PLS-2 model provided much better results than those obtained through univariate analysis, with relative errors in the range 2.2%–21.7% instead of 18.3%–163.3% and with recoveries varying from 88.8% to 121.7% instead of from 55.4% to 263.3%.

Thus, this demonstrates that the implementation of multivariate analysis in the treatment of voltammetric analysis is not limited to those systems with non-interacting analytes that result in overlapped peaks due to the proximity of their redox potential [10]. In complex systems such as the one studied in this work where all analytes provide well-separated voltammetric peaks but the sizes of these peaks are strongly dependent on the interaction between analytes, multivariate analysis can model these interactions and provide a successful quantification. Furthermore, this quantification was achieved by means of PLS-2, a simple and linear chemometric method easily accessible to anyone with some background in chemometrics. This is a clear advantage to previous works that have dealt with similar problematics by resorting to more complex linear methods (e.g. multivariate linear regression assisted by a successive projections algorithm (SPA-MLR), synergistic interval PLS) [25,26], and even non-linear chemometric methods such as artificial neural networks (ANN) [27].

4. Conclusions

Thanks to the application of a linear multivariate calibration method such as PLS, it was possible to develop a robust methodology for the simultaneous determination of the metal ions Pb(II), As(III), Cu(II), and Hg(II) in aqueous matrices, using DPASV with a commercial low-temperature SPAuE (220BT, Metrohm-Dropsens) and applying a preliminary electrochemical cleaning and activation protocol. This methodology successfully accounted for the signal distortions due to the competition of the four metals for the sites of the electrode surface, and due to the formation of intermetallic compounds such as Au–Hg–As and Au–Hg–Cu. The method presented adequate analytical figures of merit, such as good linear ranges up to 69 μg/L, with R^2 greater than 0.99, and with LODs and LOQs adequate for the determination of analytes at trace levels. Therefore, the PLS approach allowed an efficient simultaneous quantification of the four metal ions considered, comparable to other multianalyte studies in the literature (with different metals), but quite simpler, as it is based on a linear model. Moreover, the new 'rotated' 4D experimental design based on CCD allowed us to calibrate with a large diversity of concentrations in the presence of four analytes, which could be useful in similar studies.

CRediT authorship contribution statement

Juan J. Triviño: Writing – original draft, Visualization, Investigation, Formal analysis. **Clara Pérez-Ràfols:** Writing – review & editing, Writing – original draft, Supervision, Formal analysis, Conceptualization. **Núria Serrano:** Writing – review & editing, Writing – original draft, Supervision, Resources, Formal analysis, Conceptualization. **Verónica Arancibia:** Writing – review & editing. **José Manuel Díaz-Cruz:** Writing – review & editing, Writing – original draft, Supervision, Resources, Formal analysis, Conceptualization.

Declaration of competing interest

The authors declare the following financial interests/personal relationships which may be considered as potential competing interests: The authors declare the following financial interests/personal relationships which may be considered as potential competing interests: José Manuel Diaz-Cruz and Núria Serrano report financial support was provided by AEI/10.13039/501100011033/Unión Europea Next Generation EU/PRTR. Veronica Arancibia reports financial support was provided by FONDECYT-Chile. Juan José Trivino reports financial support was provided by ANID-Chile. If there are other authors, they declare that they have no known competing financial interests or personal relationships that could have appeared to influence the work reported in this paper.

Acknowledgements

Financial support by FONDECYT-Chile under Regular, Grant/Award Number: 1211637 and 1251804 (VA); ANID-Chile under National Doctoral Scholarship, Grant/Award Number: 21220946 (JJT) is fully acknowledged. This work is also supported by PID2022-136709OB-C22 funded by AEI/10.13039/501100011033/Unión European Next Generation EU/PRTR and the Generalitat of Catalunya (Project 2021 SGR 00006).

Appendix A. Supplementary data

Supplementary data to this article can be found online at https://doi.org/10.1016/j.jelechem.2026.120058.

References

[1] B. Li, X. Xie, T. Meng, X. Guo, Q. Li, Y. Yang, H. Pang, Recent advance of nanomaterials modified electrochemical sensors in the detection of heavy metal ions in food and water, Food Chem. 440 (2024) 138213, https://doi.org/10.1016/j.foodchem.2023.138213.
[2] A.A. Castañeda-Ramírez, E. Rojas-García, R. López-Medina, D.C. García-Martínez, J. Nicolás-Antúnez, A.M. Maubert-Franco, Magnetite nanoparticles into Fe-BTC MOF as adsorbent material for the remediation of metal (Cu (II), Pb (II), As (III)

and Hg (II)) ions-contaminated water, Catal. Today 394 (2022) 94–102, https://doi.org/10.1016/j.cattod.2021.11.007.
[3] C. Ariño, N. Serrano, J.M. Díaz-Cruz, M. Esteban, Voltammetric determination of metal ions beyond mercury electrodes. A review, Anal. Chim. Acta 990 (2017) 11–53, https://doi.org/10.1016/j.aca.2017.07.069.
[4] C. Ariño, C.E. Banks, A. Bobrowski, R.D. Crapnell, A. Economou, A. Królicka, J. Wang, Electrochemical stripping analysis, Nat. Rev. Methods Primers 2 (1) (2022) 62, https://doi.org/10.1038/s43586-022-00143-5.
[5] A.H.I. Ben-Bassat, A. Azrad, Intermetallic compounds formed in mixed (complex) amalgams—I. The systems: copper—mercury, zinc—mercury and copper—zinc—mercury, Electrochim. Acta 23 (1) (1978) 63–69, https://doi.org/10.1016/0013-4686(78)87034-0.
[6] N. Ivanova, The electrochemistry of intermetallic compounds: a mini-review, Electrochem. Commun. 80 (2017) 48–54, https://doi.org/10.1016/j.elecom.2017.05.008.
[7] A.J. Borrill, N.E. Reily, J.V. Macpherson, Addressing the practicalities of anodic stripping voltammetry for heavy metal detection: a tutorial review, Analyst 144 (23) (2019) 6834–6849, https://doi.org/10.1039/C9AN01437C.
[8] Y. Yang, Y. Huang, H. Luo, J. Zhao, J. Bi, G. Wu, Ion interference and elimination in electrochemical detection of heavy metals using anodic stripping voltammetry, J. Electrochem. Soc. 170 (5) (2023) 057507, https://doi.org/10.1149/1945-7111/acd1ba.
[9] D. Melucci, C. Locatelli, Multivariate calibration in differential pulse stripping voltammetry using a home-made carbon-nanotubes paste electrode, J. Electroanal. Chem. 675 (2012) 25–31, https://doi.org/10.1016/j.jelechem.2012.04.020.
[10] M. Aragó, C. Ariño, À. Dago, J.M. Díaz-Cruz, M. Esteban, Simultaneous determination of hydroquinone, catechol and resorcinol by voltammetry using graphene screen-printed electrodes and partial least squares calibration, Talanta 160 (2016) 138–143, https://doi.org/10.1016/j.talanta.2016.07.007.
[11] K. Martínez, C. Ariño, J.M. Díaz-Cruz, N. Serrano, M. Esteban, Multivariate standard addition for the analysis of overlapping voltammetric signals in the presence of matrix effects: application to the simultaneous determination of hydroquinone and catechol, Chemom. Intel. Lab. Syst. 178 (2018) 32–38, https://doi.org/10.1016/j.chemolab.2018.05.002.
[12] K. Ghanbari, M. Roushani, F. Farzadfar, H.C. Goicoechea, A.R. Jalalvand, Developing a four-dimensional voltammetry as a powerful electroanalytical methodology for simultaneous determination of three colorants in the presence of an uncalibrated interference, Chemom. Intel. Lab. Syst. 189 (2019) 27–38, https://doi.org/10.1016/j.chemolab.2019.04.001.
[13] R.J. Ferreira, T.R. Rosa, J. Ribeiro, R.C. Barthus, Simultaneous metal determination in artisanal cachaça by using voltammetry and multivariate calibration, Food Chem. 314 (2020) 126126, https://doi.org/10.1016/j.foodchem.2019.126126.
[14] PLS_Toolbox, Version 9.1, Eigenvector Research, Inc., Manson, WA USA, 2022 98831.
[15] The MathWorks, Inc. (2024). MATLAB, version 24.1.0.2578822 (R2024a). Natick, MA: The MathWorks, Inc.
[16] Miller, J.; Miller, J. Calibration methods in instrumental analysis: regression and correlation. In Statistics and Chemometrics for Analytical Chemistry; Phil Weston, Ed.; Pearson Education Limited: Harlow, England, 2010; pp. 110–153 ISBN 978-0-273-73042-2.
[17] X. Dai, R.G. Compton, Gold nanoparticle modified electrodes show a reduced interference by Cu (II) in the detection of As (III) using anodic stripping voltammetry, Electroanalysis 17 (14) (2005) 1325–1330, https://doi.org/10.1002/elan.200403246.
[18] W.Z. Zhang, K. Wang, N. Bao, S.N. Ding, Co-deposition of bimetallic au-Pt with L-cysteine on electrodes and removal of copper by Iron powder for trace aqueous arsenic detection, J. Compos. Sci. 8 (8) (2024) 327, https://doi.org/10.3390/jcs8080327.
[19] B. Kumar Jena, C. Retna Raj, Gold nanoelectrode ensembles for the simultaneous electrochemical detection of ultratrace arsenic, mercury, and copper, Anal. Chem. 80 (13) (2008) 4836–4844, https://doi.org/10.1021/ac071064w.
[20] P. Clares, C. Pérez-Ràfols, N. Serrano, J.M. Díaz-Cruz, Voltammetric determination of active pharmaceutical ingredients using screen-printed electrodes, Chemosensors 10 (3) (2022) 95, https://doi.org/10.3390/chemosensors10030095.
[21] N. Serrano, Ò. Castilla, C. Ariño, M.S. Diaz-Cruz, J.M. Díaz-Cruz, Commercial screen-printed electrodes based on carbon nanomaterials for a fast and cost-effective voltammetric determination of paracetamol, ibuprofen and caffeine in water samples, Sensors 19 (18) (2019) 4039, https://doi.org/10.3390/s19184039.
[22] V. Padilla, N. Serrano, J.M. Díaz-Cruz, Determination of trace levels of nickel (II) by adsorptive stripping voltammetry using a disposable and low-cost carbon screen-printed electrode, Chemosensors 9 (5) (2021) 94, https://doi.org/10.3390/chemosensors9050094.
[23] Wikipedia contributors. (n.d.). Rotations in 4-dimensional Euclidean space. Wikipedia. Retrieved June 6, 2025, from https://en.wikipedia.org/wiki/Rotations_in_4-dimensional_Euclidean_space.
[24] P. Carlier, What is the math required to do 4D rotations?, in: Mathematics Stack Exchange, 2024, February 1. Retrieved June 6, 2025, from, https://math.stackexchange.com/questions/4854901/what-is-the-math-required-to-do-4d-rotations.
[25] P.D. Marreto, A.M. Zimer, R.C. Faria, L.H. Mascaro, E.C. Pereira, W.D. Fragoso, S. G. Lemos, Multivariate linear regression with variable selection by a successive projections algorithm applied to the analysis of anodic stripping voltammetry data, Electrochim. Acta 127 (2014) 68–78, https://doi.org/10.1016/j.electacta.2014.02.029.
[26] L. Pinto, S.G. Lemos, Comparison of different PLS algorithms for simultaneous determination of Cd (II), Cu (II), Pb (II), and Zn (II) by anodic stripping voltammetry at bismuth film electrode, Electroanalysis 26 (2) (2014) 299–305, https://doi.org/10.1002/elan.201300500.
[27] W. Tang, J. Bin, W. Fan, Z. Zhang, Y. Yun, Y. Liang, Simultaneous determination of lead and tin at the bismuth film electrode by square wave stripping voltammetry and chemometric methods, Anal. Methods 8 (27) (2016) 5475–5486, https://doi.org/10.1039/C6AY00955G.